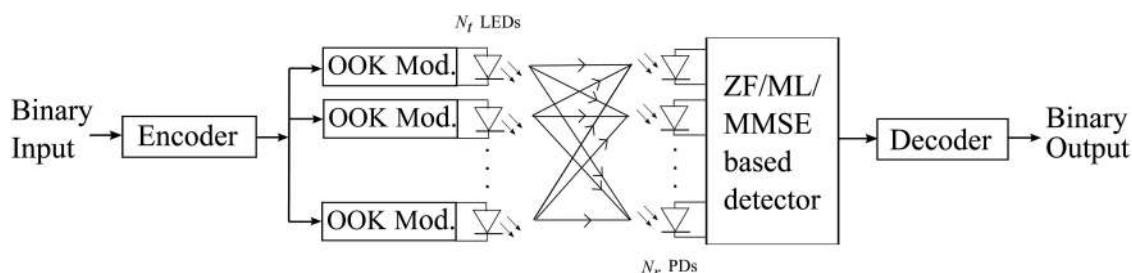# MIMO Codes for Uniform Illumination Across Space and Time in VLC With Dimming Control

Volume 11, Number 3, June 2019

Uday Thummaluri
Abhinav Kumar, *Member, IEEE*
Lakshmi Natarajan, *Member, IEEE*

IEEE

MIMO Codes for Uniform Illumination Across Space and Time in VLC With Dimming Control

Uday Thummaluri [iD]**, Abhinav Kumar, *Member, IEEE*,
and Lakshmi Natarajan** [iD]**, *Member, IEEE***

Department of Electrical Engineering, Indian Institute of Technology Hyderabad,
Hyderabad 502285 India

Abstract: Indoor visible light communications (VLC) require simultaneous illumination and communication. Hence, uniformity in the illumination is a key consideration for user comfort and data transfer in the VLC systems. Several run-length-limited codes have been proposed in the literature that mitigate flicker for single-input and single-output VLC systems. Recently, codes have been proposed for multiple-input multiple-output (MIMO) VLC systems. However, uniform illumination along with dimming control has not been considered for MIMO VLC systems. Hence, in this paper, we propose codes with generalized algorithms for encoding and decoding that maintain consistency in the illumination across space and time and achieve the desired dimming level. We present the expressions for code rate, run-length, and Hamming distance for the proposed codes. Through Monte Carlo simulations, we compare the code matrix error rate (CER) performance of the proposed codes with zero-forcing, minimum mean square error, and maximum likelihood based detectors for various number of transmit and receive antennas. We also compare the mutual information of the proposed codes for various number of transmit and receive antennas. The numerical results show that the proposed codes exhibit good performance while satisfying the design criteria.

Index Terms: Code design, code rate, code matrix error rate (CER), Hamming distance, multiple input multiple output (MIMO), mutual information, run-length, visible light communications (VLC).

1. Introduction

Nowadays, light emitting diodes (LEDs) are extensively used for indoor illumination due to their several advantages over the conventional sources of light [1]. Visible light communications (VLC) uses intensity modulation of optical sources like LEDs for wireless data transfer to achieve high data rates with little effect on perceived illumination by humans [2], [3]. Given that the same LEDs are simultaneously used for illumination and communication in VLC, the user should not perceive changes in the intensity levels while the data is being transferred. The binary stream of data to be transferred can contain large streams of zeros (assuming ON-OFF keying (OOK)) which causes flickering whenever the duration of zeros exceeds the maximum flickering time period (MFTP) of 5 ms [4], and hence, can cause discomfort to the human eyes. To mitigate this flicker effect,

several run-length limited (RLL) codes have been proposed for single input single output (SISO) VLC systems [5]–[10]. All codewords of the RLL codes may not always have equal weight [5] which can cause inconsistency in the illumination. Hence, direct current (DC) balanced codes like 4B6B code [7] have been proposed for SISO VLC systems. The DC balanced codes have equal number of zeros and ones in all of their codewords ensuring constant weight codewords. In [11]–[13], a generalized space shift keying technique and in [14], a trace-orthogonal based pulse position modulation space time block code (STBC) has been designed for multiple input multiple output (MIMO) VLC systems. In [15], a coding scheme for uniform illumination in MIMO VLC systems has been proposed. However, consistency in illumination for all the transmit antennas (LEDs) has not been considered. Novel angle diversity techniques for indoor MIMO VLC systems have been proposed in [16]. Optimal constellation design for 2×2 MIMO VLC system has been presented in [17] that results in improved error performance over the existing methods. However, consistency in illumination across different time slots has not been considered in these works. Spatial modulation schemes along with dimming control have been proposed in [18] and [19], but, uniform illumination across both space and time has not been considered in them.

Given different times of the day, different brightness levels are required in order to maintain the desired ambiance [20]. To achieve desired ambiance, dimming levels have to be controlled. For this, addition of compensation symbols at the end of the RLL codes has been proposed for VLC systems in [21]. Addition of the compensation symbols corresponding to the desired dimming level to improve the bit error rate performance has been proposed in [22]. Novel schemes to achieve desired dimming levels for SISO VLC systems have been proposed in [23], [24]. However, to the best of our knowledge this paper is the first work that jointly considers uniform illumination across space and time along with dimming control for MIMO VLC systems.

The contributions of this work are as follows.
- We propose novel code design that can be used to generate codes for MIMO VLC systems that provides uniform illumination across space and time conditioned on MFTP and maintain consistency in the illumination.
- We achieve the desired dimming levels based on the number of transmit antennas.
- We consider the code rate, run-length, code matrix error rate (CER), mutual information, and Hamming distance as the performance metrics for the proposed codes.
- We present simulation results comparing the performance of the proposed codes with zero-forcing (ZF), minimum mean square error (MMSE), and maximum likelihood (ML) based detectors for various number of transmit and receive antennas.

The organization of the paper is as follows. In Section 2, proposed system model is presented. In Section 3, the algorithm for encoding and decoding of the proposed codes is discussed. Dimming support of the proposed codes with an algorithm to generate the code matrices that achieve the desired dimming level is presented in Section 4. In Section 5, code rate, run-length, CER, mutual information, and Hamming distance are analyzed for the proposed codes. Numerical results are presented in Section 6. In Section 7, some concluding remarks along with the possible future work are discussed.

Notations: The following notations are used in this paper. We use $(.)!$, $\lfloor . \rfloor$, $||.||$, $tr(.)$, $|.|$, $(.)^T$, and $\mathbb{E}(.)$ to denote factorial operation, floor function, Frobenius norm, trace operation, determinant of a matrix, transpose operation, and expectation operation, respectively. The $Q(.)$ function is defined as $Q(w) = \frac{1}{2\pi} \int_w^\infty exp(-u^2/2)du$.

2. System Model

The schematic of the VLC system considered in this work is shown in Fig. 1. We consider a MIMO VLC system with N_t transmit antennas and N_r receive antennas. From the input bit stream at the transmitter (Tx), we assume that at a time k bit length message vector is passed through the encoder. The output of the encoder is considered to be N_t bits per time slot each of which is uniquely mapped to a Tx antenna. These bits are then OOK modulated and transmitted through the respective Tx antennas. At receiver (Rx), the received signals from the N_r Rx antennas over
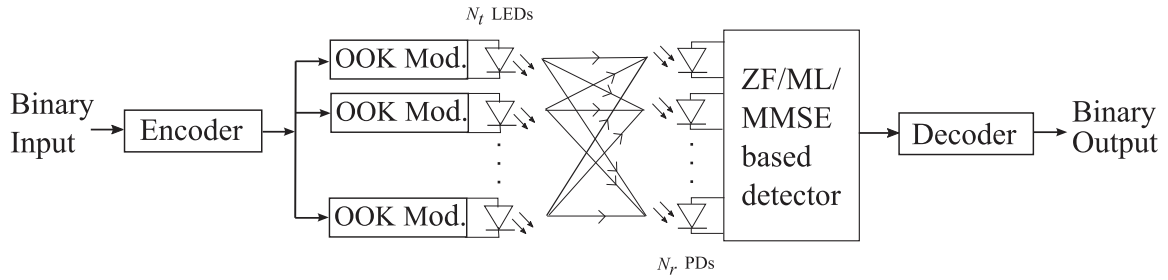
Fig. 1. Schematic of the VLC system considered.

multiple time slots are jointly passed through the detector as shown in Fig. 1. After ZF/ML/MMSE detection, the signals are processed by the decoder that generates a binary message vector of length k at a time at the Rx. Let $\underline{\mathbf{H}}$ denote the channel gain matrix given by

$$\underline{\mathbf{H}} = \begin{bmatrix} h_{11} & h_{12} & h_{13} & \dots & h_{1N_t} \\ h_{21} & h_{22} & h_{23} & \dots & h_{2N_t} \\ \vdots & \vdots & \vdots & \ddots & \vdots \\ h_{N_r1} & h_{N_r2} & h_{N_r3} & \dots & h_{N_rN_t} \end{bmatrix},$$

where, h_{ji} is the channel gain between j^{th} Rx antenna and i^{th} Tx antenna. Considering additive white Gaussian noise (AWGN) channel as in [25], the received signal, $\underline{\mathbf{Y}}$ can be represented as

$$\underline{\mathbf{Y}} = E_s \underline{\mathbf{H}} \underline{\mathbf{X}}^a + \underline{\mathbf{N}}, \tag{1}$$

where, E_s is the intensity multiplication factor of $\underline{\mathbf{X}}^a$, $\underline{\mathbf{X}}^a$ is the ath code matrix and $\underline{\mathbf{N}}$ is the independent and identically distributed (i.i.d) additive white Gaussian noise (AWGN) vector with 0 mean and co-variance matrix $\underline{\Sigma}$. We consider the following VLC channel in this work. However, the proposed codes are also valid for other VLC channel models.

2.1 VLC Channel

The DC channel gain [26] between j^{th} Rx antenna and i^{th} Tx antenna is given as

$$h_{ji} = \frac{(m+1)A R_p}{2\pi d_{ji}^2} \cos(\phi_{ji})^m T(\psi_{ji}) g(\psi_{ji}) \cos(\psi_{ji}), \tag{2}$$

where, m is the order of Lambertian radiation pattern given by $m = -1/\log_2(\cos(\Phi_{1/2}))$ such that $\Phi_{1/2}$ is the angle at half power of LED, A denotes the detection area of the photo detector (PD) at the Rx, R_p denotes the responsivity of the PD, $T(\psi_{ji})$ represents the gain of the optical filter used at the Rx, d_{ji} is the distance between the jth Rx antenna and the ith Tx antenna, ψ_{ji} is the angle as shown in Fig. 2, and $g(\psi_{ji})$ represents the gain of the optical concentrator given by

$$g(\psi_{ji}) = \begin{cases} \frac{\eta^2}{\sin(\psi_{fov})}, & 0 \le \psi_{ji} \le \psi_{fov}, \\ 0, & \psi_{ji} > \psi_{fov}, \end{cases}$$

where, η is the refractive index of the optical concentrator at the Rx and ψ_{fov} is the field of view of the photo detector at the Rx as shown in Fig. 2. Note that, just for ease of illustration, we have represented the parameters for the jth Rx antenna and i^{th} Tx antenna in Fig. 2, the same can be generalized to any Rx antenna-Tx antenna pair in the considered VLC system.
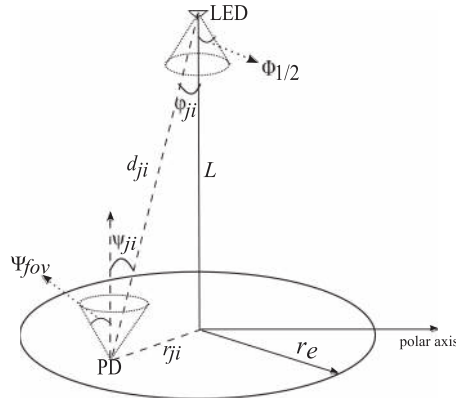
Fig. 2. Figure showing Tx antenna and Rx antenna parameters.

Considering uniform movement of the Rx in the radial direction, as in [26], the final expression for channel gain between j^{th} Rx antenna and i^{th} Tx antenna is given by

$$h_{ji} = \frac{C(m+1)L^{m+1}}{\left(r_{ji}^2 + L^2\right)^{\frac{m+3}{2}}}, \tag{3}$$

where, L is the vertical distance between i^{th} LED and the surface, r_{ji} is the radial distance between the jth Rx antenna and i^{th} Tx antenna from the top view as shown in Fig. 2, and $C = \frac{1}{2\pi} A R_p T(\psi_{ji}) g(\psi_{ji})$. Note that (2) is equivalent to (3). However, (3) allows modeling of random movement of Rx in the Rx plane. Next, we present the proposed codes with generalized algorithms.

3. Proposed Codes

Given k length message vector and N_t Tx antennas, we propose a method to map these k bits to $N_t \times N_t$ code matrix. We denote a $N_t \times N_t$ a^{th} code matrix by $\underline{\mathbf{X}}^a$, where, $a \in \{0, 1, \ldots, 2^k - 1\}$ such that

$$\underline{\mathbf{X}}^a = \begin{bmatrix} x_{11}^a & x_{12}^a & x_{13}^a & \cdots & x_{1\,N_t-1}^a & x_{1\,N_t}^a \\ x_{21}^a & x_{22}^a & x_{23}^a & \cdots & x_{2\,N_t-1}^a & x_{2\,N_t}^a \\ \vdots & \vdots & \vdots & \ddots & \vdots & \vdots \\ x_{N_t-1\,1}^a & x_{N_t-1\,2}^a & x_{N_t-1\,3}^a & \cdots & x_{N_t-1\,N_t-1}^a & x_{N_t-1\,N_t}^a \\ x_{N_t\,1}^a & x_{N_t\,2}^a & x_{N_t\,3}^a & \cdots & x_{N_t\,N_t-1}^a & x_{N_t\,N_t}^a \end{bmatrix},$$

where, x_{js}^a denotes the bit at j^{th} Tx antenna in the sth time slot of the ath code matrix and $x_{js}^a \in \{0, 1\}$. We first propose codes for minimum possible dimming factor denoted by γ and then generalize them for various achievable dimming factors, for a given N_t. Traditionally, in single Tx antenna VLC systems, as in [22], the dimming factor has been defined as the proportion of time the Tx antenna is ON while transmitting a codeword. However, in MIMO VLC systems the dimming factor can be defined as the proportion of total ON time of all Tx antennas while transmitting a code matrix. Hence, we define γ as

$$\gamma = \frac{\text{Total number of 1 s in the code matrix}}{\text{Total number of bits in the code matrix}}. \tag{4}$$

To ensure constant dimming level, the γ should not change between code matrices. To ensure uniformity in illumination across different Tx antennas, each of the Tx antenna should be ON for
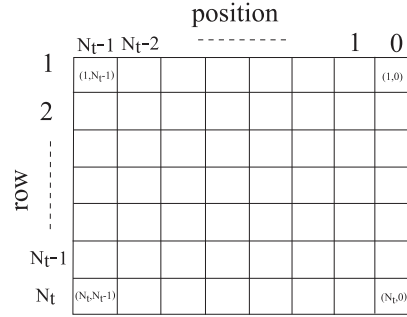
Fig. 3. Format of the code matrix showing row number and position of 1 s.

same proportion of time. Thus, each row of the code matrix should have the same weight for a given N_t. Similarly, to ensure uniform illumination by the N_t Tx antennas across different time slots, each column of the code matrix should have the same weight. Thus, the requirement of uniform illumination across time slots and across Tx antennas results in the following two constraints

$$\sum_{s=1}^{N_t} x_{sj}^a = M, \forall j \in \{1, 2, \ldots, N_t\}, \tag{5}$$

$$\sum_{j=1}^{N_t} x_{sj}^a = M, \forall s \in \{1, 2, \ldots, N_t\}, \tag{6}$$

where, M should be equal to γN_t. The minimum possible value of M is 1. Hence, using (4), (5), and (6), minimum possible value of γ that can be achieved with uniform illumination is given as

$$\gamma = \frac{1}{N_t}.$$

The γ and E_s in (1) can be varied simultaneously to achieve desired illumination. It is observed from (5) and (6) that dimming achieved across different time slots and Tx antennas is same at code matrix level.

We first consider the code design for M = 1, i.e., $\gamma = 1/N_t$. We will generalize this code design for various possible dimming factors in the next section. The proposed algorithm maps every k bits for a given N_t to a unique code matrix that has exactly one 1 in each row and each column. For example, a $N_t \times N_t$ identity matrix is a valid code matrix if it satisfies (5), and (6). A code matrix generated by this method will maintain uniformity in the illumination over space and time. The positions of 1 s in the code matrix are decided by considering Fig. 3. The column indices are considered from right to left and row indices are considered form top to bottom. Consider the following lemma, where, the possibility for unique mapping of message vectors to code matrices is discussed.

Lemma 1: If $P_i = \lfloor R_i/(N_t - i)! \rfloor$, $1 \leq i \leq N_t$ and $R_i = R_{i-1} \bmod (N_t - i + 1)!$, $2 \leq i \leq N_t$, $0 \leq R_1 \leq 2^{N_t} - 1$, *then the set of P_is denoted by $\{P_i\}$ will differ in at least one value for every distinct R_1, where, P_is and R_is are integers.*

Proof: See Appendix A for the proof.

Let the code matrix be $\underline{\mathbf{X}}^a$, R_1 be the decimal equivalent of the k binary bits, R_i be the integer for the ith row and P_i be the position of 1 in the ith row. Then, for 1st row the position of 1 is calculated

as below

$$(N_t - 1).(N_t - 2).(N_t - 3)\ldots 3.2.1.\ P_1 \leq R_1,$$

$$(N_t - 1)!P_1 \leq R_1,$$

$$P_1 = \lfloor R_1/(N_t - 1)! \rfloor ,$$

$$x^a_{1\,pos} = \begin{cases} 1, & \text{if } pos = P_1 \\ 0, & \text{otherwise,} \end{cases}$$

$$\text{where, } pos \in \{0, 1, \ldots (N_t - 1)\}.$$

For any other row, i.e., i^{th} row and $i \leq N_t$, the position of 1 s is given as

$$R_i = R_{i-1} \bmod ((N_t - i + 1).(N_t - i).(N_t - i - 1)\ldots 3.2.1),$$

$$R_i = R_{i-1} \bmod (N_t - i + 1)!,$$

$$(N_t - i).(N_t - i - 1).(N_t - i - 2)\ldots 3.\ 2.\ 1.\ P_i \leq R_i,$$

$$(N_t - i)!P_i \leq R_i,$$

$$P_i = \lfloor R_i/(N_t - i)! \rfloor .$$

In case there are 1 s in the previous rows whose position is less than or equal to the current position, then increment the current P_i by that many number of positions. During this increment process, if any position of 1 s in the previous rows become less than or equal to the P_i in the increment process, then the increment for that positions also should be considered.

$$x^a_{i\,pos} = \begin{cases} 1, & \text{if } pos = P_i \\ 0, & \text{otherwise,} \end{cases}$$

$$\text{where, } i \in \{2 \ldots N_t\}.$$

The code matrices generated by Algorithm 1 are given in Appendix B for N_t equal to 4. Decoding the code matrix to get back the message is done post detection of the received noisy version of the code matrix. Here, we find the actual positions, i.e., the values of P_i ($i \geq 2$) which are calculated at step 10 in Algorithm 1 by decreasing the position index as many times as the number of 1 s on the right hand side of the current 1 in the rows above the current row in the code matrix. Since 1st row does not have any rows above it, position of 1 can be found directly. These actual positions can be directly used to recover the decimal equivalent corresponding to binary message vector of length k as shown in Algorithm 2. (*Note: If the binary equivalent has lesser length than k, append 0 s on the left hand side till it's length becomes k.*). Next, we present the proposed algorithm for dimming control.

4. Dimming Control With the Proposed Codes

The proposed code design can also be used for dimming control [27], [28]. The proposed codes can achieve any dimming of the kind f/N_t, where, $f \in \{1, 2, \ldots, N_t - 1\}$. To achieve dimming corresponding to the dimming factor $1 - (1/N_t)$, the code matrices generated by the proposed encoder can be directly complemented. To achieve any other dimming, consider Algorithm 3.

The code matrices generated by Algorithm 3 are given in Appendix B for N_t equal to 4 and γ equal to 0.5 and 0.75. Let $Wt_{\gamma actual}(\mathbf{X}^a)$ be the weight of the code matrix output of the proposed algorithm and $Wt_{\gamma desired}(\mathbf{X}^a)$ be the weight of the code matrix which achieves desired γ per Tx antenna. $Wt_{\gamma actual}(\mathbf{X}^a) = N_t$ and $Wt_{\gamma desired}(\mathbf{X}^a) = \gamma N_t^2$. The relation between $Wt_{\gamma actual}(\mathbf{X}^a)$ and $Wt_{\gamma desired}$

Algorithm 1: Algorithm For Encoding.

1: INPUT: The number of Tx antennas, N_t.
2: OUTPUT: N_t x N_t code matrix.
3: Find the optimal value of message vector length, k using constraint.
4: From the binary stream of data each k bits are considered at a time and they are converted to equivalent decimal values.
5: Let R_1 be the integer initially corresponding to k bits, P_i be the position of 1 in the ith row, R_i be the integer for the ith row.
6: Initializations: Let val $= N_t - 1$, $P_1 = \lfloor R_1 / \text{val}! \rfloor$.
7: **for** i $= 2$ to N_t **do**
8:     $R_i = R_{i-1} \mod \text{val}!$
9:     val $= $ val $- 1$
10:    $P_i = \lfloor R_i / \text{val}! \rfloor$
11:    If there are 1 s in the previous rows whose position is less than or equal to the current position, then increment the current P_i by that many number of positions. If any position of 1 s in the previous rows become less than or equal to the P_i in the increment process, then the increment for that positions also should be considered.
12:    Update the code matrix here.
13: **end for**
14: Code matrix corresponding to the input k length message vector is generated.

Algorithm 2: Algorithm For Decoding.

1: INPUT: Received code matrix, $\underline{Y}$.
2: OUTPUT: Decoded binary output.
3: Find the locations of 1 in the received vector after detection. Let pos_vec be the vector containing the position of 1 s in the code matrix to be decoded.
4: Initializations: pos_vec1(1) = pos_vec(1) % *pos_vec1 contains the actual position values*.
5: **for** r $= 2$ to N_t **do**
6:     var0 $= 0$
7:     **for** t $= r - 1$ to 1 (decrease) **do**
8:         **if** pos_vec(r) > pos_vec(t) **then**
9:             var0++
10:        **end if**
11:    **end for**
12:    pos_vec1(r) = pos_vec(r)-var0
13: **end for**
14: dec_val $= 0$ and var1 $= N_t - 1$
15: **for** r $= 1$ to N_t **do**
16:    dec_val = dec_val + var1! $\times$ pos_vec1(r)
17:    var1- -
18: **end for**
19: Convert dec_val to binary to get the message back.

---

is given as

$$Wt_{\gamma desired}(\underline{\mathbf{X}}^a) = \gamma \left(Wt_{\gamma actual}(\underline{\mathbf{X}}^a) \right)^2 . \tag{7}$$

Since actual code matrices and their complemented version represents the lower and upper bounds on the achievable dimming for given N_t, few comparisons and relation corresponding to them are given below.

TABLE 1

Complemented Vs Actual Codes

N_t	γ_{actual}	γ_c	$Wt_{\gamma_{actual}}(\underline{\mathbf{X}}^a)$	$Wt_c(\underline{\mathbf{X}}^a)$
4	0.2500	0.750	4	12
5	0.2000	0.800	5	20
6	0.1667	0.833	6	30
7	0.1428	0.857	7	42
8	0.1250	0.875	8	56

Algorithm 3: Algorithm to Achieve Dimming.

1: INPUT: code matrix corresponding to $\gamma = 1/N_t$ i.e., the output of Algorithm 1 and the other input required is desired γ in the possible range which is $2/N_t \leq \gamma \leq (N_t - 2)/N_t$.

2: OUTPUT: code matrix corresponding the desired γ per Tx antenna.

3: Find the number of 1 s that are required to achieve the given γ excluding the one 1 which is already present. This number is given by $f = \gamma N_t - 1$.

4: **for** `r = 1 to` N_t **do**

5:     Find the location of 1 in r^{th} row of the code matrix taken.

6:     Replace f 0 s which are on the right hand side of the 1 with ones.

7:     If location of replacement exceeds the code matrix dimension, start replacing from first location.

8: **end for**

Let the code matrices generated by the proposed Algorithm 1 be the actual code matrices. Let γ_{actual} be the dimming factor per antenna for the actual version and γ_c be the dimming factor per antenna for the complemented version. Then, $\gamma_{actual} = 1/N_t$ and $\gamma_c = 1 - (1/N_t)$. Let the weight of the code matrix for the complemented version of the code matrices be $Wt_c(\underline{\mathbf{X}}^a)$. Then, the relation between $Wt_{\gamma_{actual}}(\underline{\mathbf{X}}^a)$ and $Wt_c(\underline{\mathbf{X}}^a)$ is given as follows

$$Wt_{\gamma_{actual}}(\underline{\mathbf{X}}^a) = N_t,$$

$$Wt_c(\underline{\mathbf{X}}^a) = N_t^2 - N_t,$$

$$Wt_c(\underline{\mathbf{X}}^a) = N_t(N_t - 1),$$

$$Wt_c(\underline{\mathbf{X}}^a) = Wt_{\gamma_{actual}}(\underline{\mathbf{X}}^a)(Wt_{\gamma_{actual}}(\underline{\mathbf{X}}^a) - 1).$$

Consider Table 1, where, complemented and actual versions are compared for few values of N_t. Next, we present the performance metrics considered for analyzing the proposed codes.

5. Performance Analysis

In this section, the performance of the proposed codes is analyzed in terms of code rate, run-length, code matrix error rate, mutual information, and minimum Hamming distance.

5.1 Code Rate

For M = 1, from (6), each Tx antenna is ON exactly for one time slot in a code matrix. Hence, for N_t Tx antennas, we have $N_t!$ combinations of code matrices that satisfy (5) and (6). Given message vector length as k bits, the total possible combinations of the message vectors is 2^k. Each of the message vectors has to be uniquely mapped to a code matrix. Hence, we have the following constraint
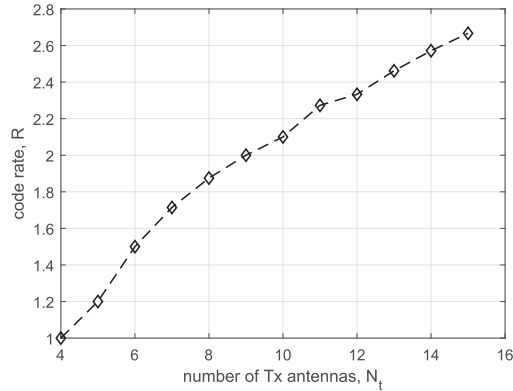
$$2^k \leq N_t!. \tag{8}$$

Fig. 4. Variation of code rate with respect to number of Tx antennas, N_t for the proposed codes.

The code rate is typically defined as the number of bits transmitted per time slot [29]. Hence, for the proposed codes, the code rate denoted by R will be equal to k/N_t. Thus, to maximize code rate, using (8), we have $k = \lfloor \log_2(N_t!) \rfloor$ and

$$R = \frac{\lfloor \log_2(N_t!) \rfloor}{N_t}.$$

Note that for the proposed codes, the code rate increases with N_t as shown in Fig. 4 and to achieve higher code rates, larger LED arrays can be used at Tx as in [30].

5.2 Run-Length

The run-length of the proposed codes is defined per Tx antenna. In VLC context, run-length is defined as the number of continuous 0 s in the binary stream of data. Hence, for MIMO codes, run-length is defined per Tx antenna. For the actual version of the codes, i.e., codes generated by Algorithm 1, maximum run-length is $2N_t - 2$ which can be seen from the format of the code matrices and for the complemented version of the codes, the maximum run-length is always 2 irrespective of the value of N_t. Consider the following example code matrices for different values of γ for the proposed codes for $N_t = 4$.

Example:

$$\underline{\mathbf{X}}^a(\gamma = 0.25) = \begin{bmatrix} 0 & 0 & 0 & 1 \\ 0 & 0 & 1 & 0 \\ 0 & 1 & 0 & 0 \\ 1 & 0 & 0 & 0 \end{bmatrix},$$

$$\underline{\mathbf{X}}^a(\gamma = 0.50) = \begin{bmatrix} 1 & 0 & 0 & 1 \\ 0 & 0 & 1 & 1 \\ 0 & 1 & 1 & 0 \\ 1 & 1 & 0 & 0 \end{bmatrix},$$

$$\underline{\mathbf{X}}^a(\gamma = 0.75) = \begin{bmatrix} 1 & 1 & 0 & 1 \\ 1 & 0 & 1 & 1 \\ 0 & 1 & 1 & 1 \\ 1 & 1 & 1 & 0 \end{bmatrix}.$$

The $\underline{\mathbf{X}}^a(\gamma = 0.25)$ can give a maximum run-length of 6 if the code matrix shown in the example is transmitted first, and the next transmitted code matrix has 0001 for 4th Tx antenna and accordingly

TABLE 2

Upper Bound on N_t to Achieve Minimum Possible Dimming

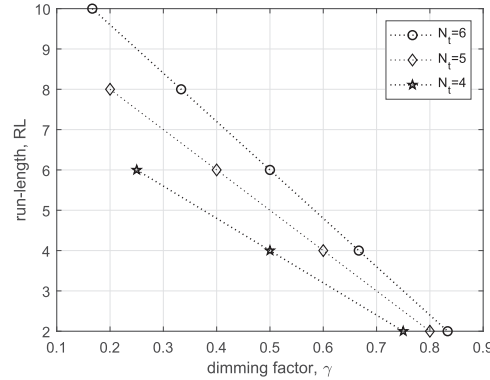| T_b	N_t
0.2 ms	13
0.1 ms	26
50 μs	51
20 μs	126
1 μs	2501

Fig. 5. Run-length per Tx antenna by varying γ.

for the other Tx antennas. The $\underline{\mathbf{X}}^a(\gamma = 0.75)$ can give a maximum run-length of 2 if the code matrix shown in the example is transmitted first, and the next transmitted code matrix has 0111 for 4th Tx antenna and accordingly for the other Tx antennas. Similarly, for given N_t and from Algorithm 3 which helps in achieving desired γ, the run-length for any desired and possible γ is given as

$$RL = 2N_t - 2\gamma N_t,$$
$$= 2N_t(1 - \gamma). \tag{9}$$

Maximum possible run-length occurs when the dimming level is least for a given N_t. Consider Table 2, where, the value of N_t is calculated for few values of T_b.

A flicker is a change in intensity and is observed in a VLC system whenever the duration of 0 s exceeds the time corresponding to MFTP. The MFTP is defined as the maximum time period over which the change in light intensity is not perceived by the human eye. The MFTP for human eye is 5ms or frequency less than 200 Hz [4]. For the proposed codes, given N_t number of Tx antennas, maximum run-length is $N_t - 1$ per Tx antenna in a code matrix, and hence, $2(N_t - 1)$ in the data stream transmitted by any Tx antenna. Maximum run-length for given N_t occurs for least possible γ (M = 1).

Let T_b be the time period of a bit, either 0 or 1. For given N_t and for maximum possible run-length, to avoid flickering, the relation between MFTP and T_b of the proposed codes is given as

$$(2N_t - 2) T_b < MFTP. \tag{10}$$

Then, from (10) the upper bound on the value of N_t is given by the following equation

$$N_t = \left\lfloor \frac{MFTP + 2T_b}{2T_b} \right\rfloor. \tag{11}$$

In Fig. 5, for given N_t, RL s are compared for all possible values of γ using (9). In Fig. 6, maximum possible RL (for $\gamma = 1/N_t$) for given N_t are compared.
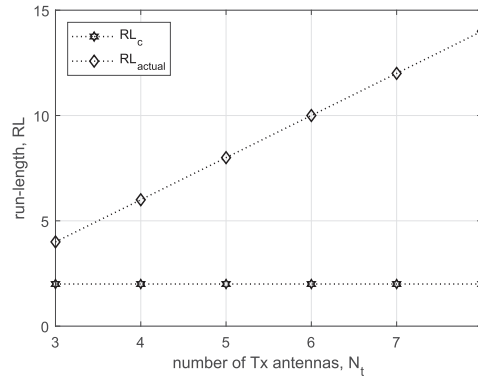
Fig. 6. Run-length per Tx antenna for complemented and actual version of the proposed codes.

5.3 Code Matrix Error Rate (CER)

Union bound on CER is calculated using pairwise error probability (PEP) [31]. The expression for CER is given as

$$CER \leq \mathbb{E}_{\underline{\mathbf{H}}}\left(\frac{2}{2^k} \sum_{a=0}^{2^k-2} \sum_{b=a+1}^{2^k-1} PEP(\underline{\mathbf{X}}^a, \underline{\mathbf{X}}^b) \right), \tag{12}$$

where, $\mathbb{E}_{\underline{\mathbf{H}}}$ denotes expectation over channel gain matrix and $PEP(\underline{\mathbf{X}}^a, \underline{\mathbf{X}}^b)$ denotes PEP between two code matrices $\underline{\mathbf{X}}^a$ and $\underline{\mathbf{X}}^b$ ($a \neq b$). Then, the expression for PEP can be calculated as shown below

$$PEP(\underline{\mathbf{X}}^a, \underline{\mathbf{X}}^b) = Pr\left\{ ||\underline{\mathbf{Y}} - E_s\underline{\mathbf{H}}\,\underline{\mathbf{X}}^a||^2 > ||\underline{\mathbf{Y}} - E_s\underline{\mathbf{H}}\,\underline{\mathbf{X}}^b||^2 \Big| \underline{\mathbf{X}}^a \right\}.$$

By substituting $\underline{\mathbf{Y}} = E_s\underline{\mathbf{H}}\,\underline{\mathbf{X}}^a + \underline{\mathbf{N}}$, the expression can be evaluated as

$$PEP(\underline{\mathbf{X}}^a, \underline{\mathbf{X}}^b) = Q\left(\frac{E_s||\underline{\mathbf{H}}(\mathbf{X}^a - \mathbf{X}^b)||}{\sqrt{2N_0}} \right). \tag{13}$$

By substituting (13) in (12), the final expression in $Q(.)$ function can be given as follows

$$CER \leq \frac{1}{2^{k-1}} \sum_{a=0}^{2^k-2} \sum_{b=a+1}^{2^k-1} \mathbb{E}_{\underline{\mathbf{H}}}\left(Q\left(E_s\sqrt{\frac{||\mathbf{H}(\mathbf{X}^a - \mathbf{X}^b)||^2}{2N_0}} \right) \right).$$

In the above expression of CER, $||\underline{\mathbf{H}}(\mathbf{X}^a - \mathbf{X}^b)||^2$ is given by

$$||\underline{\mathbf{H}}(\mathbf{X}^a - \mathbf{X}^b)||^2 = \sum_{s=1}^{N_t} \sum_{j=1}^{N_r} \left| \sum_{i=1}^{N_t} h_{ji}\left(x_{is}^a - x_{is}^b\right) \right|^2,$$

where, x_{is}^a denotes value in i^{th} row and the sth column of the ath code matrix.

5.4 Mutual Information

Let $I(\underline{\mathbf{X}}^a; \underline{\mathbf{Y}}|\underline{\mathbf{H}})$ be the mutual information between $\underline{\mathbf{X}}^a$ and $\underline{\mathbf{Y}}$ given the channel gain matrix $\underline{\mathbf{H}}$. The number of channel uses is same as the number of Tx antennas from the code design. Then, for N_t channel uses, the mutual information [32] is given as

$$I(\underline{\mathbf{X}}^a; \underline{\mathbf{Y}}|\underline{\mathbf{H}}) = \frac{1}{N_t} \left(h(\underline{\mathbf{Y}}|\underline{\mathbf{H}}) - h(\underline{\mathbf{Y}}|\underline{\mathbf{H}}, \underline{\mathbf{X}}^a) \right), \tag{14}$$

where, $h(.)$ is the differential entropy function. For given $\underline{\mathbf{H}}$, $\underline{\mathbf{X}}^a$, $h(\underline{\mathbf{Y}}|\underline{\mathbf{H}}, \underline{\mathbf{X}}^a)$ is given by the following equation

$$h(\underline{\mathbf{Y}}|\underline{\mathbf{H}}, \underline{\mathbf{X}}^a) = h((E_s\underline{\mathbf{H}}\,\underline{\mathbf{X}}^a + \underline{\mathbf{N}})|\underline{\mathbf{H}}, \underline{\mathbf{X}}^a),$$

$$= h(\underline{\mathbf{N}}).$$

Since $\underline{\mathbf{N}}$ has the dimensions $N_r \times N_t$ and AWGN is considered, $h(\underline{\mathbf{N}})$ has to be calculated using matrix normal distribution. Probability density function (pdf) of matrix normal distribution [33], [34] is given as

$$\mathcal{MN}_{(n,p)} = \frac{exp\left(\frac{1}{2}tr\left(\underline{\mathbf{V}}^{-1}(\underline{\mathbf{S}}-\underline{\mathbf{B}})^T\underline{\mathbf{U}}^{-1}(\underline{\mathbf{S}}-\underline{\mathbf{B}})\right)\right)}{(2\pi)^{np/2}|\underline{\mathbf{V}}|^{n/2}|\underline{\mathbf{U}}|^{p/2}}. \tag{15}$$

In (15), $\underline{\mathbf{S}}$ is the Gaussian random matrix of dimensions $n \times p$, $\underline{\mathbf{B}}$ is the mean matrix of dimensions $n \times p$, $\underline{\mathbf{V}}$ is the scale matrix of dimensions $n \times n$, and $\underline{\mathbf{U}}$ is the scale matrix of dimensions $p \times p$. From the assumption of i.i.d. noise components, the expression for $h(\underline{\mathbf{N}})$ can be computed as follows

$$h(\underline{\mathbf{N}}) = \frac{1}{2}\log_2\left((2\pi e)^{N_tN_r}|\underline{\Sigma}|^{N_t}\right). \tag{16}$$

Considering uniform distribution for code matrices, the weight of each Gaussian is equal and hence, the final expression for mutual information using (14), (15), and (16) can be evaluated as follows

$$I\left(\underline{\mathbf{X}}^a; \underline{\mathbf{Y}}|\underline{\mathbf{H}}\right) = \frac{1}{N_t}\left(\mathbb{E}\left(\log_2\left(\frac{1}{f(y|\underline{\mathbf{H}})}\right)\right) - \frac{1}{2}\log_2\left((2\pi e)^{N_tN_r}|\underline{\Sigma}|^{N_t}\right)\right),$$

and

$$f(y|\underline{\mathbf{H}}) = \frac{\sum_{\underline{\mathbf{X}}^a \epsilon \mathcal{X}} exp\left(-\frac{1}{2}tr\left((\underline{\mathbf{Y}} - E_s\underline{\mathbf{H}}\,\underline{\mathbf{X}}^a)^T\underline{\Sigma}^{-1}(\underline{\mathbf{Y}} - E_s\underline{\mathbf{H}}\,\underline{\mathbf{X}}^a)\right)\right)}{(2\pi)^{N_tN_r/2}2^k|\underline{\Sigma}|^{N_t/2}},$$

where, $f(.)$ is the pdf of y given $\underline{\mathbf{H}}$, and $\mathcal{X}$ is the set of all code matrices for given N_t and γ.

5.5 Minimum Hamming Distance

Since the output of the proposed encoder is binary code matrices, we consider minimum Hamming distance as the performance metric. However, minimum Euclidean distance can also be considered as the code matrices are intensity modulated before transmission. Let d_{min} be the minimum Hamming distance between any pair of code matrices $\underline{\mathbf{X}}^a$ and $\underline{\mathbf{X}}^b$ ($a \neq b$). Let $\underline{\mathbf{X}}^a$ be denoted as

$$\underline{\mathbf{X}}^a = \begin{bmatrix} \underline{X}^a_1 \\ \underline{X}^a_2 \\ \underline{X}^a_3 \\ \vdots \\ \underline{X}^a_{N_t} \end{bmatrix},$$

where, $\underline{X}^a_i$ denotes the ith row of the ath code matrix. The d_{min} is first computed for $\gamma = 1/N_t$ and then, it is generalized for achievable arbitrary γ whose range is conditioned on N_t. By the design of the codes each row and each column of any code matrix has only one 1, i.e., each code matrix is a permutation matrix. Let $\underline{\mathbf{X}}^a$ be the first code matrix and $\underline{\mathbf{X}}^b$ be the second code matrix which is formed by swapping exactly two rows of $\underline{\mathbf{X}}^a$. Let l be the position of 1 in $\underline{X}^a_i$ and l' be the position of

1 in $\underline{X}_j^a$ and $l \neq l'$. One such case can be shown as follows

$$\mathbf{X}^a = \begin{bmatrix} \underline{X}_1^a \\ \underline{X}_2^a \\ \underline{X}_3^a \\ \vdots \\ \underline{X}_{N_t-1}^a \\ \underline{X}_{N_t}^a \end{bmatrix}, \ \mathbf{X}^b = \begin{bmatrix} \underline{X}_1^b \\ \underline{X}_2^b \\ \underline{X}_3^b \\ \vdots \\ \underline{X}_{N_t-1}^b \\ \underline{X}_{N_t}^b \end{bmatrix},$$

where, $\underline{X}_1^b = \underline{X}_1^a$, $\underline{X}_2^b = \underline{X}_2^a$, ..., $\underline{X}_{N_t-1}^b = \underline{X}_{N_t}^a$, $\underline{X}_{N_t}^a = \underline{X}_{N_t-1}^a$. Now, let $\underline{X}_{N_t-1}^a = [0\,0\,\ldots\,0\,0\,1\,0\,0\,\ldots\,0\,0]$, $\underline{X}_{N_t}^a = [0\,0\,\ldots\,0\,0\,0\,1\,0\,\ldots\,0\,0]$. Then,

$$d_{min} = 2\left(Wt(\underline{X}_i^a) + Wt(\underline{X}_j^a)\right),$$

$$= 2(1+1),$$

$$= 4.$$

Similarly, for arbitrary γ say $\gamma = q/N_t$ where $2 \leq q \leq N_t - 1$ and from Step 6 and 7 of Algorithm 3 which says about the position of 1 s to achieve desired γ. Consider the following example. Let $\underline{X}_i^a = [0\,0\,\ldots\,0\,0\,1\,1\,1\,\ldots\,1\,1\,0\,0\,\ldots\,0]$, $\underline{X}_j^a = [0\,0\,\ldots\,0\,0\,0\,1\,1\,\ldots\,1\,1\,1\,0\,\ldots\,0]$. Then, d_{min} can be given as below

$$d_{min} = 2\left(Wt(\underline{X}_i^a) + Wt(\underline{X}_j^a)\right) - 4(\text{number of 1 s common to both the rows}),$$

$$= 2\left(Wt(\underline{X}_i^a) + Wt(\underline{X}_j^a)\right) - 4(\gamma N_t - 1),$$

$$= 2\left(\gamma N_t + \gamma N_t\right) - 4(\gamma N_t - 1),$$

$$= 4\gamma N_t - 4\gamma N_t + 4,$$

$$= 4.$$

Therefore, the d_{min} for the proposed codes is 4. Similarly, it can be shown that the minimum Euclidean distance for the proposed codes is $2E_s$. Next, we present numerical results comparing various cases of proposed codes.

6. Numerical Results

For generating numerical results we consider the following system configuration. However, the proposed codes are valid for any other system configuration. Assuming circular area of coverage, the top view of the system can be shown as in Fig. 7. All the Tx antennas are assumed to be placed at equal distance from the center of the Tx, T_0. The Rx is assumed to move uniformly in the coverage area with the Rx plane horizontal to the surface and with constant orientation as shown in Fig. 7. Let center of the surface be (0,0) i.e., the position of T_0 from the top view. Let T_i denote the ith Tx antenna and R_i denote the ith Rx antenna. The distance between T_0 and T_i for $i \geq 1$ be l' and the distance between R_0 and R_i for $i \geq 1$ be l.

For 4 Tx antennas case, the Tx antennas assumed are T_i for $1 \leq i \leq 4$. This is done just to maintain the symmetry in the VLC system. For the same case with a Rx antennas ($a \leq 4$), they are R_i for $1 \leq i \leq a$. For 5 Tx antennas case the 5th Tx antenna is taken to be T_0 and for 5th Rx antenna, it is taken at R_0. Let (c_i, d_i) be the position of R_i. In the proposed work, the reference point for the Rx is taken to be R_0 whose co-ordinates are calculated from the independent and uniformly distributed r and θ which are shown in Fig. 7. From the preceding considerations the position of any Rx antenna can be calculated using simple trigonometry analysis as follows.

The position of R_0 is given as (c_0, d_0), where, $c_0 = r\cos\theta$ and $d_0 = r\sin\theta$. The position of R_1 is given as (c_1, d_1), where, $c_1 = c_0 + l$ and $d_1 = d_0$. The position of R_2 is given as (c_2, d_2), where, $c_2 = c_0$ and
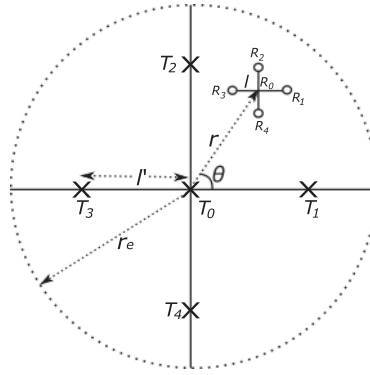
Fig. 7. Top view of the scenario considered.

$d_2 = d_0 + l$. The position of R_3 is given as (c_3, d_3), where, $c_3 = c_0 - l$ and $d_3 = d_0$. Similarly, $c_4 = c_0$ and $d_4 = d_0 - l$ gives the position of R_4. Note that the boundary for R_0 is taken to be r_e, but some Rx antennas beyond R_0 can be outside the boundary.

Assuming all LEDs are identical and all PDs are identical, the parameters [26] for simulation are as follows:- Vertical distance from LEDs to surface, L is 2.15 m, cell radius, r_e is 3.55 m, LED semi angle $\Phi_{1/2}$ and PD FOV, ψ_{fov} are both 60°, PD responsivity, R_p is 0.4 A/W, PD detection area, A is 1 cm², refractive index, $\eta = 1.5$, optical filter gain, T is 1, distance from the reference point of the Tx to each Tx antenna, l' is 1 m, and distance from the reference point of the Rx to each Rx antenna, l is 5 cm. Since Tx antenna positions are fixed, from the above considerations, their locations on co-ordinate axes in meters is given as (1, 0), (0, 1), (−1, 0), and (0, −1) for the Tx antennas T_1, T_2, T_3, and T_4, respectively. For $N_t = 5$, T_0 is considered to be the 5th Tx antenna whose location is the reference point itself, i.e., (0,0). The r, θ are generated from the uniform distributions, $U[0, r_e]$ and $U[0, 2\pi)$, respectively. The $R_0 = (c_0, d_0) = (r\cos\theta, r\sin\theta)$ acts as the reference point for the Rx. Since distance between the reference point of the Rx to other Rx antennas is l and assumed to be 5 cm, ie., 0.05 m. Then, $R_1 = (c_1, d_1) = (c_0 + 0.05, d_0)$, $R_2 = (c_2, d_2) = (c_0, d_0 + 0.05)$, $R_3 = (c_3, d_3) = (c_0 - 0.05, d_0)$, and $R_4 = (c_4, d_4) = (c_0, d_0 - 0.05)$. For 5 Rx antennas case, another Rx antenna is considered at R_0. Similar Tx and Rx structures can be designed for any N_t and N_r. Here we will assume that the Rx has the knowledge of the γ used at the Tx. For the proposed codes, CER simulation results are presented for ML, MMSE, and ZF based detectors. In ML detection, we minimize the Euclidean distance over all possible code matrices and the ML detection rule is given as

$$\hat{\underline{X}}_{ML}^a = \min_{\forall \underline{X}^a} ||\underline{Y} - E_s \underline{H}\,\underline{X}^a||^2 \; \forall \; \underline{X}^a.$$

In numerical results, to compare the CER and mutual information for different values of γ, any constellation used in this paper is properly normalized such that the average energy transmitted per code matrix, $\gamma E_s N_t^2$ remains the same. This can be done by tuning E_s. In the following plots SNR in dB is equal to $\gamma E_s N_t^2 / N_0$. Note that the indoor VLC typically operates at high SNR due to strong line of sight component and short propagation distances [35]. In Figs. 8 and 9, the CER plots using simulation along with union bound are shown for 4 Tx antennas-1 Rx antenna, 4 Tx antennas-2 Rx antennas and 4 Tx antennas-4 Rx antennas cases for $\gamma = 0.25$ and $\gamma = 0.75$, respectively using ML detection. Form Figs. 8 and 9, it can be seen that as γ increases CER performance decreases for same number of Tx antennas and same number of Rx antennas cases. In MMSE detection, the estimate of $\underline{Y}$ denoted by $\hat{\underline{X}}_{MMSE}^a$ is given as

$$\hat{\underline{X}}_{MMSE}^a = \left(\underline{H}^T + \frac{N_0}{2}\underline{I}\right)^{-1} \underline{H}^T \underline{Y},$$
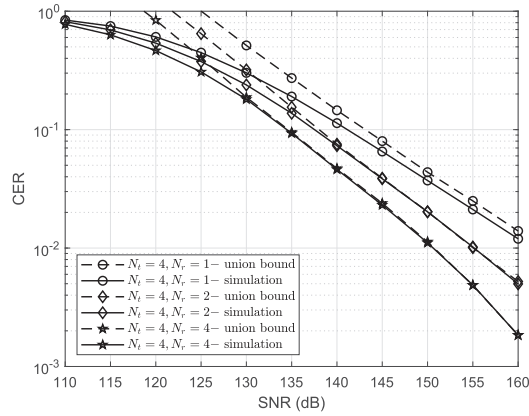
Fig. 8. CER plots for 4 Tx antennas and varying number of Rx antennas with union bound for $\gamma = 0.25$.
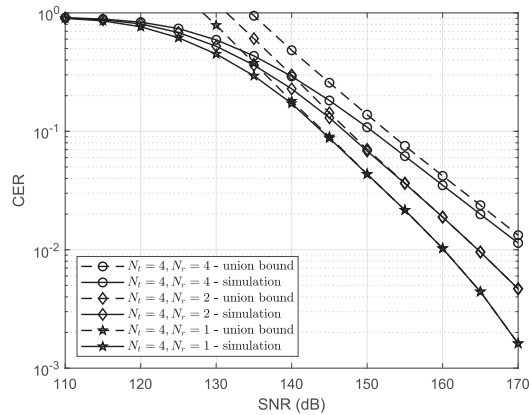

Fig. 9. CER plots for 4 Tx antennas and varying number of Rx antennas with union bound for $\gamma = 0.75$.

and for ZF detection, the estimate of $\underline{\mathbf{Y}}$ denoted by $\hat{\underline{\mathbf{X}}}_{ZF}$ is given as

$$\hat{\underline{\mathbf{X}}}_{ZF}^{a} = \underline{\mathbf{H}}^{-1}\underline{\mathbf{Y}}.$$

Since $1/N_t \leq \gamma \leq (N_t - 1)/N_t$, to decode any received vector after ZF and MMSE detection, take f number of higher magnitude values in each row of the matrix to be 1 and remaining to be 0 if the γ used at the transmitter is f/N_t, where, $f \in \{1, 2, \ldots, N_t - 1\}$. At this point, if $\hat{\underline{\mathbf{X}}}_{ZF}^{a}$ or $\tilde{\underline{\mathbf{X}}}_{MMSE}^{a}$ is not a valid code matrix, we randomly choose a message vector as the decoded vector.

Remark 1: Since the proposed algorithm is systematic, we need not exhaustively search over all the code matrices at the Tx. Further, at the Rx side also, the exhaustive search can be avoided with ZF and MMSE based detectors. The memory required to store a lookup table for the code matrices can be saved both at Tx and Rx whose value increases with increase in N_t. Thus, the proposed code has reduced complexity, while maintaining the error rate below a predetermined threshold.

In Figs. 10 and 11, CER plots are shown for ZF, MMSE and ML based detectors for 4 Tx antennas and 4 Rx antennas case for $\gamma = 0.25$, $\gamma = 0.75$ and for 5 Tx antennas and 5 Rx antennas case for $\gamma = 0.20$, $\gamma = 0.80$, respectively. In Fig. 12, the CERs for 5 Tx antennas and varying number of Rx antennas case for $\gamma = 0.2$ and 0.8 are compared where the effect of dimming and number of receive antennas on the system performance is observed. In Fig. 13, the mutual information plots for 4 Tx antennas and 1, 2, 3 and 4 Rx antennas are shown. Similarly in Fig. 14, the mutual information plots for 5 Tx antennas and 1, 2, 3, 4 and 5 Rx antennas are shown. It can be seen
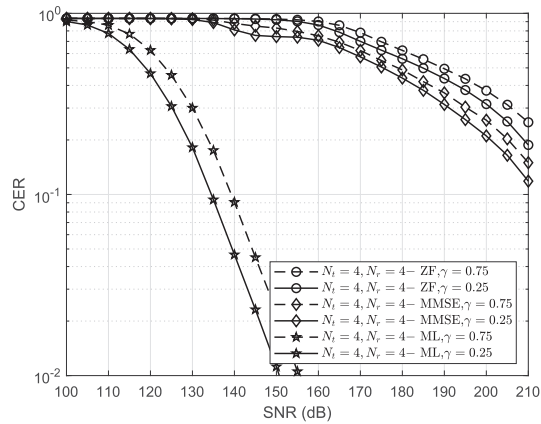
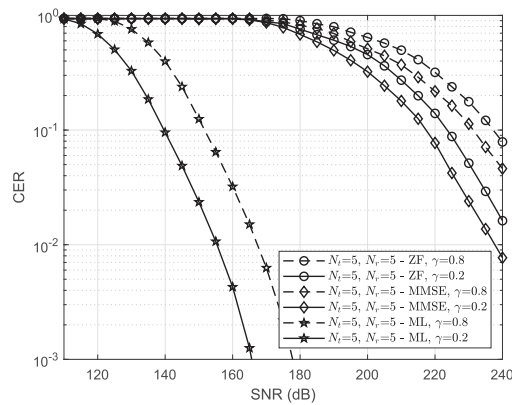Fig. 10. CER plots for 4 Tx antennas and 4 Rx antennas with ZF, MMSE and ML based detectors.

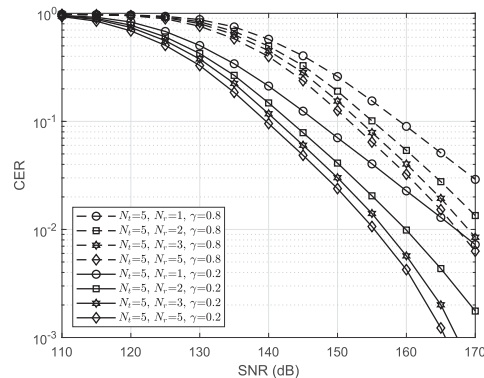Fig. 11. CER plots for 5 Tx antennas and 5 Rx antennas with ZF, MMSE and ML based detectors.

Fig. 12. CER plots for 5 Tx antennas and varying number of Rx antennas.

that, the mutual information increases as the number of Rx antennas increase before it saturates to the code rate. The difference in the code rates achieved is seen from the saturation levels in the mutual information plots. The code rates achieved by 4 Tx antennas and 5 Tx antennas cases are 1.0 bit/slot and 1.2 bits/slot, respectively.
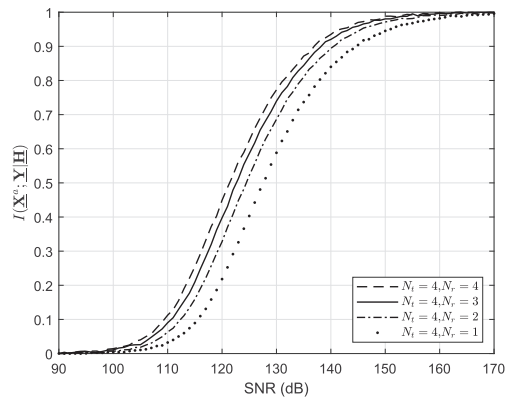
Fig. 13. Mutual information plots for 4 Tx antennas and varying number of Rx antennas for $\gamma = 0.25$.
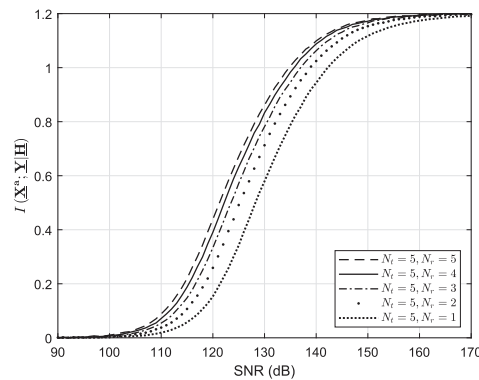

Fig. 14. Mutual information plots for 5 Tx antennas and varying number of Rx antennas for $\gamma = 0.20$.
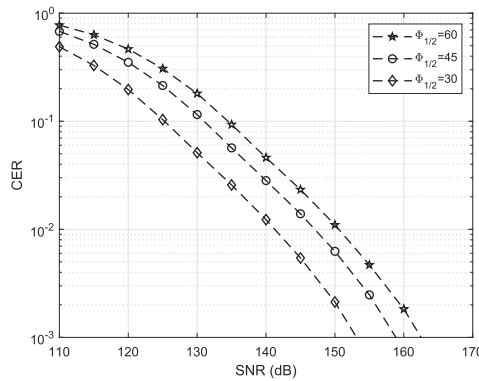

Fig. 15. CER plots for 4 Tx antennas and 4 Rx antennas for three values of semi angle of LED (in degrees), $\Phi_{1/2}$ for $\gamma = 0.25$.

In Fig. 15, the effect of $\Phi_{1/2}$ on CER performance is shown. From (2), it is observed that channel gain increases as $\Phi_{1/2}$ decreases, and hence, there is an improvement in CER performance with reduction in $\Phi_{1/2}$. Some concluding remarks and possible future work are discussed in the next section.

7. Conclusion

We have proposed codes with generalized algorithms for encoding, decoding, and to achieve desired dimming. We have discussed the rates achieved, run-lengths for least dimming level achieved conditioned on MFTP. We have presented CER plots for different number of transmit and receive antennas with different dimming levels along with the mathematical expressions for union bound. We have also presented the plots for mutual information along with the expressions. We have shown the minimum Hamming distance for the proposed codes. Since the proposed codes do not perform well in the low SNR regions, they are suitable for scenarios like indoor VLC where the SNRs are typically high due to line of sight and shorter distances. In future, we plan to test the performance of the proposed codes on hardware.

Appendix A

The Lemma 1 is proved by assuming two numbers w and $w + z$, $z \neq 0$ such that both the numbers lie between 0 and $2^{N_t} - 1$. Let $R_1 = w$ such that $0 \leq R_1 \leq 2^{N_t} - 1$. Then,

$$P_1^w = \left\lfloor \frac{R_1}{(N_t - 1)!} \right\rfloor,$$

$$P_2^w = \left\lfloor \frac{w \bmod (N_t - 1)!}{(N_t - 2)!} \right\rfloor,$$

$$P_3^w = \left\lfloor \frac{(w \bmod (N_t - 1)!) \bmod (N_t - 2)!}{(N_t - 3)!} \right\rfloor.$$

Similarly, $(N_t - 2)^{th}$ term is given as

$$P_{N_t-2}^w = \left\lfloor \frac{((w \bmod (N_t - 1)!) \bmod (N_t - 2)! \ldots) 3!}{2!} \right\rfloor.$$

Further, when $R_1 = w + z$ and $z \neq 0$, P_is are given as

$$P_1^{w+z} = \left\lfloor \frac{R_1}{(N_t - 1)!} \right\rfloor,$$

$$P_2^{w+z} = \left\lfloor \frac{(w + z) \bmod (N_t - 1)!}{(N_t - 2)!} \right\rfloor,$$

$$P_3^{w+z} = \left\lfloor \frac{((w + z) \bmod (N_t - 1)!) \bmod (N_t - 2)!}{(N_t - 3)!} \right\rfloor.$$

Similarly, $(N_t - 2)^{th}$ term is given as

$$P_{N_t-2}^{w+z} = \left\lfloor \frac{(((w + z) \bmod (N_t - 1)!) \bmod (N_t - 2)! \ldots) 3!}{2!} \right\rfloor.$$

Let us assume the P_is are same for both w and $w + z$ till $i = N_t - 3$. For the $(N_t - 2)^{th}$ value of P_i, it is seen that the modulo operation in the numerator is done with 3! at the end. So the numerator value at this stage lies among $\{0, 1, 2, 3, 4, 5\}$. This value is divided by 2! and floored to get P_{N_t-2} which can be $\{0, 0, 1, 1, 2, 2\}$, respectively. If w and $w + z$ leave different P_i at this place, then the Lemma 1 statement is satisfied. If P_{N_t-2} is same for both w and $w + z$ then they differ in the $(N_t - 1)^{th}$ and N_t^{th} P_is because of the distinct R_is. In brief, at $(N_t - 2)^{th}$ P_i, the R_i is found using modulo with 3!. If the two numbers, w and $w + z$ are such that they give different remainders when divided by 6, they differ in P_is at that step itself otherwise in the later steps. Similar explanation

holds true for any P_{N_t-i}, and hence, $\{P_i\}$ has at least one element not in common for $z \neq 0$. This concludes the proof of Lemma 1. ∎

Appendix B

The code matrices for mapping 0 to 15 for $\gamma = 0.25$ and $N_t = 4$ are as follows.

$$
\begin{bmatrix} 0 & 0 & 0 & 1 \\ 0 & 0 & 1 & 0 \\ 0 & 1 & 0 & 0 \\ 1 & 0 & 0 & 0 \end{bmatrix},
\begin{bmatrix} 0 & 0 & 0 & 1 \\ 0 & 0 & 1 & 0 \\ 1 & 0 & 0 & 0 \\ 0 & 1 & 0 & 0 \end{bmatrix},
\begin{bmatrix} 0 & 0 & 0 & 1 \\ 0 & 1 & 0 & 0 \\ 0 & 0 & 1 & 0 \\ 1 & 0 & 0 & 0 \end{bmatrix},
\begin{bmatrix} 0 & 0 & 0 & 1 \\ 0 & 1 & 0 & 0 \\ 1 & 0 & 0 & 0 \\ 0 & 0 & 1 & 0 \end{bmatrix},
$$

$$
\begin{bmatrix} 0 & 0 & 0 & 1 \\ 1 & 0 & 0 & 0 \\ 0 & 0 & 1 & 0 \\ 0 & 1 & 0 & 0 \end{bmatrix},
\begin{bmatrix} 0 & 0 & 0 & 1 \\ 1 & 0 & 0 & 0 \\ 0 & 1 & 0 & 0 \\ 0 & 0 & 1 & 0 \end{bmatrix},
\begin{bmatrix} 0 & 0 & 1 & 0 \\ 0 & 0 & 0 & 1 \\ 0 & 1 & 0 & 0 \\ 1 & 0 & 0 & 0 \end{bmatrix},
\begin{bmatrix} 0 & 0 & 1 & 0 \\ 0 & 0 & 0 & 1 \\ 1 & 0 & 0 & 0 \\ 0 & 1 & 0 & 0 \end{bmatrix},
$$

$$
\begin{bmatrix} 0 & 0 & 1 & 0 \\ 0 & 1 & 0 & 0 \\ 0 & 0 & 0 & 1 \\ 1 & 0 & 0 & 0 \end{bmatrix},
\begin{bmatrix} 0 & 0 & 1 & 0 \\ 0 & 1 & 0 & 0 \\ 1 & 0 & 0 & 0 \\ 0 & 0 & 0 & 1 \end{bmatrix},
\begin{bmatrix} 0 & 0 & 1 & 0 \\ 1 & 0 & 0 & 0 \\ 0 & 0 & 0 & 1 \\ 0 & 1 & 0 & 0 \end{bmatrix},
\begin{bmatrix} 0 & 0 & 1 & 0 \\ 1 & 0 & 0 & 0 \\ 0 & 1 & 0 & 0 \\ 0 & 0 & 0 & 1 \end{bmatrix},
$$

$$
\begin{bmatrix} 0 & 1 & 0 & 0 \\ 0 & 0 & 0 & 1 \\ 0 & 0 & 1 & 0 \\ 1 & 0 & 0 & 0 \end{bmatrix},
\begin{bmatrix} 0 & 1 & 0 & 0 \\ 0 & 0 & 0 & 1 \\ 1 & 0 & 0 & 0 \\ 0 & 0 & 1 & 0 \end{bmatrix},
\begin{bmatrix} 0 & 1 & 0 & 0 \\ 0 & 0 & 1 & 0 \\ 0 & 0 & 0 & 1 \\ 1 & 0 & 0 & 0 \end{bmatrix},
\begin{bmatrix} 0 & 1 & 0 & 0 \\ 0 & 0 & 1 & 0 \\ 1 & 0 & 0 & 0 \\ 0 & 0 & 0 & 1 \end{bmatrix}.
$$

The code matrices for mapping 0 to 15 for $\gamma = 0.50$ and $N_t = 4$ are as follows.

$$
\begin{bmatrix} 1 & 0 & 0 & 1 \\ 0 & 0 & 1 & 1 \\ 0 & 1 & 1 & 0 \\ 1 & 1 & 0 & 0 \end{bmatrix},
\begin{bmatrix} 1 & 0 & 0 & 1 \\ 0 & 0 & 1 & 1 \\ 1 & 1 & 0 & 0 \\ 0 & 1 & 1 & 0 \end{bmatrix},
\begin{bmatrix} 1 & 0 & 0 & 1 \\ 0 & 1 & 1 & 0 \\ 0 & 0 & 1 & 1 \\ 1 & 1 & 0 & 0 \end{bmatrix},
\begin{bmatrix} 1 & 0 & 0 & 1 \\ 0 & 1 & 1 & 0 \\ 1 & 1 & 0 & 0 \\ 0 & 0 & 1 & 1 \end{bmatrix},
$$

$$
\begin{bmatrix} 1 & 0 & 0 & 1 \\ 1 & 1 & 0 & 0 \\ 0 & 0 & 1 & 1 \\ 0 & 1 & 1 & 0 \end{bmatrix},
\begin{bmatrix} 1 & 0 & 0 & 1 \\ 1 & 1 & 0 & 0 \\ 0 & 1 & 1 & 0 \\ 0 & 0 & 1 & 1 \end{bmatrix},
\begin{bmatrix} 0 & 0 & 1 & 1 \\ 1 & 0 & 0 & 1 \\ 0 & 1 & 1 & 0 \\ 1 & 1 & 0 & 0 \end{bmatrix},
\begin{bmatrix} 0 & 0 & 1 & 1 \\ 1 & 0 & 0 & 1 \\ 1 & 1 & 0 & 0 \\ 0 & 1 & 1 & 0 \end{bmatrix},
$$

$$
\begin{bmatrix} 0 & 0 & 1 & 1 \\ 0 & 1 & 1 & 0 \\ 1 & 0 & 0 & 1 \\ 1 & 1 & 0 & 0 \end{bmatrix},
\begin{bmatrix} 0 & 0 & 1 & 1 \\ 0 & 1 & 1 & 0 \\ 1 & 1 & 0 & 0 \\ 1 & 0 & 0 & 1 \end{bmatrix},
\begin{bmatrix} 0 & 0 & 1 & 1 \\ 1 & 1 & 0 & 0 \\ 1 & 0 & 0 & 1 \\ 0 & 1 & 1 & 0 \end{bmatrix},
\begin{bmatrix} 0 & 0 & 1 & 1 \\ 1 & 1 & 0 & 0 \\ 0 & 1 & 1 & 0 \\ 1 & 0 & 0 & 1 \end{bmatrix},
$$

$$\begin{bmatrix} 0 & 1 & 1 & 0 \\ 1 & 0 & 0 & 1 \\ 0 & 0 & 1 & 1 \\ 1 & 1 & 0 & 0 \end{bmatrix}, \begin{bmatrix} 0 & 1 & 1 & 0 \\ 1 & 0 & 0 & 1 \\ 1 & 1 & 0 & 0 \\ 0 & 0 & 1 & 1 \end{bmatrix}, \begin{bmatrix} 0 & 1 & 1 & 0 \\ 0 & 0 & 1 & 1 \\ 1 & 0 & 0 & 1 \\ 1 & 1 & 0 & 0 \end{bmatrix}, \begin{bmatrix} 0 & 1 & 1 & 0 \\ 0 & 0 & 1 & 1 \\ 1 & 1 & 0 & 0 \\ 1 & 0 & 0 & 1 \end{bmatrix}.$$

The code matrices for mapping 0 to 15 for $\gamma = 0.75$ and $N_t = 4$ are as follows.

$$\begin{bmatrix} 1 & 1 & 0 & 1 \\ 1 & 0 & 1 & 1 \\ 0 & 1 & 1 & 1 \\ 1 & 1 & 1 & 0 \end{bmatrix}, \begin{bmatrix} 1 & 1 & 0 & 1 \\ 1 & 0 & 1 & 1 \\ 1 & 1 & 1 & 0 \\ 0 & 1 & 1 & 1 \end{bmatrix}, \begin{bmatrix} 1 & 1 & 0 & 1 \\ 0 & 1 & 1 & 1 \\ 1 & 0 & 1 & 1 \\ 1 & 1 & 1 & 0 \end{bmatrix}, \begin{bmatrix} 1 & 1 & 0 & 1 \\ 0 & 1 & 1 & 1 \\ 1 & 1 & 1 & 0 \\ 1 & 0 & 1 & 1 \end{bmatrix},$$

$$\begin{bmatrix} 1 & 1 & 0 & 1 \\ 1 & 1 & 1 & 0 \\ 1 & 0 & 1 & 1 \\ 0 & 1 & 1 & 1 \end{bmatrix}, \begin{bmatrix} 1 & 1 & 0 & 1 \\ 1 & 1 & 1 & 0 \\ 0 & 1 & 1 & 1 \\ 1 & 0 & 1 & 1 \end{bmatrix}, \begin{bmatrix} 1 & 0 & 1 & 1 \\ 1 & 1 & 0 & 1 \\ 0 & 1 & 1 & 1 \\ 1 & 1 & 1 & 0 \end{bmatrix}, \begin{bmatrix} 1 & 0 & 1 & 1 \\ 1 & 1 & 0 & 1 \\ 1 & 1 & 1 & 0 \\ 0 & 1 & 1 & 1 \end{bmatrix},$$

$$\begin{bmatrix} 1 & 0 & 1 & 1 \\ 0 & 1 & 1 & 1 \\ 1 & 1 & 0 & 1 \\ 1 & 1 & 1 & 0 \end{bmatrix}, \begin{bmatrix} 1 & 0 & 1 & 1 \\ 0 & 1 & 1 & 1 \\ 1 & 1 & 1 & 0 \\ 1 & 1 & 0 & 1 \end{bmatrix}, \begin{bmatrix} 1 & 0 & 1 & 1 \\ 1 & 1 & 1 & 0 \\ 1 & 1 & 0 & 1 \\ 0 & 1 & 1 & 1 \end{bmatrix}, \begin{bmatrix} 1 & 0 & 1 & 1 \\ 1 & 1 & 1 & 0 \\ 0 & 1 & 1 & 1 \\ 1 & 1 & 0 & 1 \end{bmatrix},$$

$$\begin{bmatrix} 0 & 1 & 1 & 1 \\ 1 & 1 & 0 & 1 \\ 1 & 0 & 1 & 1 \\ 1 & 1 & 1 & 0 \end{bmatrix}, \begin{bmatrix} 0 & 1 & 1 & 1 \\ 1 & 1 & 0 & 1 \\ 1 & 1 & 1 & 0 \\ 1 & 0 & 1 & 1 \end{bmatrix}, \begin{bmatrix} 0 & 1 & 1 & 1 \\ 1 & 0 & 1 & 1 \\ 1 & 1 & 0 & 1 \\ 1 & 1 & 1 & 0 \end{bmatrix}, \begin{bmatrix} 0 & 1 & 1 & 1 \\ 1 & 0 & 1 & 1 \\ 1 & 1 & 1 & 0 \\ 1 & 1 & 0 & 1 \end{bmatrix}.$$

References

[1] D. Karunatilaka, F. Zafar, V. Kalavally, and R. Parthiban, "LED based indoor visible light communications: State of the art," *IEEE Commun. Surv. Tut.*, vol. 17, no. 3, pp. 1649–1678, Jul.–Sep. 2015.

[2] H. Elgala, R. Mesleh, and H. Haas, "Indoor optical wireless communication: Potential and state-of-the-art," *IEEE Commun. Mag.*, vol. 49, no. 9, pp. 56–62, Sep. 2011.

[3] S. Zhang *et al.*, "1.5 Gbit/s multi-channel visible light communications using CMOS-controlled GaN-based LEDs," *J. Lightw. Technol.*, vol. 31, no. 8, pp. 1211–1216, Apr. 2013.

[4] S. Rajagopal, R. D. Roberts, and S. K. Lim, "IEEE 802.15.7 visible light communication: modulation schemes and dimming support," *IEEE Commun. Mag.*, vol. 50, no. 3, pp. 72–82, Mar. 2012.

[5] K. Kim, K. Lee, and K. Lee, "Appropriate RLL coding scheme for effective dimming control in VLC," *Electron. Lett.*, vol. 52, no. 19, pp. 1622–1624, Sep. 2016.

[6] C. E. Mejia, C. N. Georghiades, M. M. Abdallah, and Y. H. Al-Badarneh, "Code design for flicker mitigation in visible light communications using finite state machines," *IEEE Trans. Commun.*, vol. 65, no. 5, pp. 2091–2100, May 2017.

[7] *IEEE Standard for Local and Metropolitan Area Networks—Part 15.7: Short-Range Wireless Optical Communication Using Visible Light*, IEEE Standard 802.15.7, Sep. 2011.

[8] K. Kim, K. Lee, and K. Lee, "Zero reduction codes for efficient transmission and enhanced brightness in visible light communication," *IET Optoelectronics*, vol. 11, no. 3, pp. 108–113, Jun. 2017.

[9] T. Uday, A. Kumar, and L. Natarajan, "Generation of perfectly DC balanced codes for visible light communications," in *Proc. Nat. Conf. Commun.*, Hyderabad, India, 2018, pp. 1–5.

[10] T. Uday, A. Kumar, and L. Natarajan, "Flicker mitigating high rate RLL codes for VLC with low complexity encoding and decoding," in *Proc. IEEE Int. Symp. Smart Electron. Syst.*, Hyderabad, India, 2018, pp. 1–6.

[11] R. Bian *et al.*, "Experimental demonstration of generalised space shift keying for visible light communication," in *Proc. IEEE Int. Black Sea Conf. Commun. Netw.*, Istanbul, 2017, pp. 1–5.

[12] W. O. Popoola and H. Haas, "Demonstration of the merit and limitation of generalised space shift keying for indoor visible light communications," *J. Lightw. Technol.*, vol. 32, no. 10, pp. 1960–1965, May 2014.

[13] W. O. Popoola, E. Poves, and H. Haas, "Error performance of generalised space shift keying for indoor visible light communications," *IEEE Trans. Commun.*, vol. 61, no. 5, pp. 1968–1976, May 2013.

[14] M. Biagi, A. M. Vegni, S. Pergoloni, P. M. Butala, and T. D. C. Little, "Trace-orthogonal PPM-space time block coding under rate constraints for visible light communication," *J. Lightw. Technol.*, vol. 33, no. 2, pp. 481–494, Jan. 2015.

[15] T. Uday, A. Kumar, and L. Natarajan, "Low PAPR coding scheme for uniform illumination in MIMO VLC," in *Proc. IEEE Global Commun. Conf.*, Abu Dhabi, UAE, 2018, pp. 1–6.

[16] A. Nuwanpriya, S. W. Ho, and C. S. Chen, "Indoor MIMO visible light communications: Novel angle diversity receivers for mobile users," *IEEE J. Sel. Areas Commun.*, vol. 33, no. 9, pp. 1780–1792, Sep. 2015.

[17] H. B. Cai, J. Zhang, Y. J. Zhu, J. K. Zhang, and X. Yang, "Optimal constellation design for indoor 2×2 MIMO visible light communications," *IEEE Commun. Lett.*, vol. 20, no. 2, pp. 264-267, Feb. 2016.

[18] Y. Yang, Z. Zeng, J. Cheng, and C. Guo, "Spatial dimming scheme for optical OFDM based visible light communication," *Opt. Exp.*, vol. 24, pp. 30254–30263, 2016.

[19] B. W. Kim and S.-Y. Jung, "Dimmable spatial intensity modulation for visible-light communication: Capacity analysis and practical design," *Current Opt. Photon.*, vol. 2, pp. 532–539, 2018.

[20] J. Gancarz, H. Elgala, and T. D. C. Little, "Impact of lighting requirements on VLC systems," *IEEE Commun. Mag.*, vol. 51, no. 12, pp. 34–41, Dec. 2013.

[21] H. Wang and S. Kim, "Dimming control systems with polar codes in visible light communication," *IEEE Photon. Technol. Lett.*, vol. 29, no. 19, pp. 1651–1654, Oct. 2017.

[22] T. Uday, A. Kumar, and L. Natarajan, "Improved run length limited codes for VLC using dimming control compensation symbols," in *Proc. Int. Conf. Commun. Syst. Netw.*, Bengaluru, India, 2018, pp. 457–460.

[23] S. Kim and S. Y. Jung, "Modified Reed-Muller coding scheme made from the bent function for dimmable visible light communications," *Photon. Technol. Lett.*, vol. 25, no. 1, pp. 11–13, Jan. 2013.

[24] S. Kim and S. Y. Jung, "Novel FEC coding scheme for dimmable visible light communication based on the modified Reed-Muller codes," *IEEE Photon. Technol. Lett.*, vol. 23, no. 20, pp. 1514–1516, Oct. 2011.

[25] J. H. Yoo, B. W. Kim, and S. Y. Jung, "Modelling and analysis of M-ary variable pulse position modulation for visible light communications," *IET Optoelectronics*, vol. 9, no. 5, pp. 184–190, 10 2015.

[26] L. Yin, W. O. Popoola, X. Wu, and H. Haas, "Performance evaluation of non-orthogonal multiple access in visible light communication," *IEEE Trans. Commun.*, vol. 64, no. 12, pp. 5162–5175, Dec. 2016.

[27] T. Zhang, J. Zhou, Z. Zhang, Y. Lu, F. Su, and Y. Qiao, "Dimming control systems based on low-PAPR SCFDM for visible light communications," *IEEE Photon. J.*, vol. 10, no. 5, Oct. 2018, Art no. 7907211.

[28] Y. Zuo, J. Zhang, Y. Zhang, and R. Chen, "Weight threshold check coding for dimmable indoor visible light communication systems," *IEEE Photon. J.*, vol. 10, no. 3, 2018, Art no. 7904811.

[29] K. P. Srinath and B. S. Rajan, "Generalized silver codes," *IEEE Trans. Inf. Theory*, vol. 57, no. 9, pp. 6134–6147, Sep. 2011.

[30] K. Xu, H. Yu, and Y. Zhu, "Channel-adapted spatial modulation for massive MIMO visible light communications," *IEEE Photon. Technol. Lett.*, vol. 28, no. 23, pp. 2693–2696, Dec. 2016.

[31] J. Yuan, Z. Chen, B. Vucetic, and W. Firmanto, "Performance and design of space-time coding in fading channels," *IEEE Trans. Commun.*, vol. 51, no. 12, pp. 1991–1996, Dec. 2003.

[32] T. Cover and J. Thomas, *Elements of information theory* (Wiley Series in Telecommunications), Hoboken, NJ, USA: Wiley, 1991.

[33] Dutilleul, "The MLE algorithm for the matrix normal distribution," *J. Statist. Comput. Simul.*, vol. 64, no. 2, pp. 105–123, 1999.

[34] S. F. Arnold, *The Theory of Linear Models and Multivariate Analysis*. New York, NY, USA: Wiley, 1981.

[35] H. Marshoud, P. C. Sofotasios, S. Muhaidat, G. K. Karagiannidis, and B. S. Sharif, "On the performance of visible light communication systems with non-orthogonal multiple access," *IEEE Trans. Wireless Commun.*, vol. 16, no. 10, pp. 6350–6364, Oct. 2017.